

Numerical Comparison of Pavement Distress Due to Moving Load under Dual-wheel Tandem and Tridem Axles

Ali Mansourkhaki¹, Sadegh Yeganeh*², Alireza Sarkar³

Received: 03.11.2013

Accepted: 23.09.2013

Abstract

Finite element method in pavement analysis is a type of mechanistic analysis that has widely been used by road and transportation engineers these days. This method is used with related programs such as ABAQUS/CAE which is one of the powerful software on this task. Modeling in this software has been developed from 2D static models to 3D dynamic models which are closer to reality due to the more precise definition of material properties. A 3D model of a three layered pavement system has been studied in this paper. Viscoelastic behavior definition for asphalt concrete (AC) layer which is loaded by “Dual-wheel Tandem” and “Tridem” axles has been modeled in ABAQUS/CAE. These axles are moving with different velocities. Since the model is a flexible pavement, two important structural damages are “Fatigue Cracking” and “Rutting”. In order to calculate the allowable number of load repetition to prevent each of those distresses, the horizontal tensile strain under the hot mixed asphalt (HMA) layer and vertical compressive strain on top of the subgrade are needed. The concentration of this study is based on the responses of flexible pavement. Moreover, a comparison due to moving “Dual-wheel Tandem” and “Tridem” axles loading with different velocities is made. The parameters used for comparison are the allowable numbers of load repetition to prevent “Fatigue Cracking” and “Rutting”. Due to the comparison between two configurations of axles and their speed two conclusions have been made. Stresses reduce with increase in speed up to 100km/h under two axle configurations. Also, the allowable number of Tridem axle passages to prevent Fatigue Cracking and Rutting is higher under Dual-wheel Tandem configuration.

Keywords: Axles comparison, moving load, finite element method, viscoelastic behavior, flexible pavement.

*Corresponding author E-Mail: sadegh.yegane@gmail.com

1- Associate Professor, Department of Civil Engineering, Iran University of Science and Technology, Tehran, Iran

2- MSc. Graduated from Iran University of Science and Technology, Tehran, Iran

3- Ph.D. Graduated from Iran University of Science and Technology, Tehran, Iran

Research Fellow, Faculty of Engineering, Kashan Branch, Islamic Azad University, Kashan, Iran

1. Introduction

The 1960 is the memento of AASHO's expensive road test and its impressive effects on pavements design in road and transportation engineering; that huge test was an example of empirical analysis which is known in versus of mechanistic method. Studying the effects of loading axle type on HMA layer damage, and determining the equivalent coefficients for each axle type, was one of the important achievements of that huge test. These results have been used until now. The effect of loading axle type on HMA layer damage is one of the most important parameters for pavements structural design which is applied by Equivalent Axle Load Factor (EALF). This factor defines the damage per pass to a pavement by the axle in question relative to the damage per pass of a standard axle load, usually the 18-kip (80-kN) single-axle load. Actually the design is based on the total number of the passed standard axle load during the design period, defined as the cumulative Equivalent Single-Axle Load (ESAL). Most of the EALFs in use today are based on experience. One of the most widely used methods is based on the empirical equations developed from the AASHTO Road Test. This factor can also be determined theoretically based on the critical stresses and strains in the pavement, and the failure criteria [Huang, 2004].

Mechanistic methods in computing pavements responses have received great attention at the First International Conference on Struc-

tural Design of Asphalt Pavement in 1962. The success of a mechanistic procedure mainly depends on how realistic it can model the pavement-vehicle interaction and pavement's layers material behavior. When an axle moves on the surface, it applies a dynamic load beside the static load. In conventional pavement design models, the load is assumed static and stationary; which ignores the dynamic effects of moving load. The field measured responses of pavement have clearly indicated that the speed of axle affects the pavement strain responses [Sebbaly and Tabatabaee 1993; Akram et al. 1992]. In general, there are two important factors which should be considered in any dynamic pavement analysis: the variation of the interaction load with time and the dependency of the material properties on the applied loading repetition.

In 1990, Chen et al. worked on the effect of high inflation pressure and heavy axle load on asphalt concrete pavement performance, by using 3D finite element model. A program TEXGAP-3D (developed with Abaqus), was selected to predict the performance of flexible pavements [Chen et al. 1990]. A 3D pavement with viscoelastic AC layer was modeled in Abaqus by Zaghoul and White (1993). They applied many realistic assumptions and worked on the optimum and suitable dimensions of the model's parts such as layer's depth and width. Furthermore, they applied a moving load and used dynamic analysis [Zaghoul and White, 1993]. Several studies have been

done on the optimum dimensions of pavement length, width and layers' depth for 3D modeling and finite element method [Uddin et al. 1994; Dondi 1994; Hjelmstad et al. 1997]. In 1998, a study by focusing on the usefulness of the finite element method on the analysis of three layered pavement system subjected to different types of loadings was done. Various factors such as axle type, axle load, tire pressure, vehicle speed and pavement types were examined and different material behaviors were also considered. Saad et al. (2005) examined the dynamic responses of conventional flexible pavement structures to single wheel loading in terms of fatigue strain at the bottom of the AC layer and rutting strain on the top of the subgrade material. This study conducted with 3D finite element software called ADINA [Saad et al. 2005]. In 2006, Elseifi and his team studied the hot mix asphalt viscoelastic properties at moderate and high temperature. They used this property into a 3D finite element model so that the simulated pavement responses become more accurate due to the different speed loading. Outputs of this model were compared with field measured pavement responses and the results of this analysis indicated that the elastic theory has underestimated predictions. In addition, results of the finite element model had higher correlation with field measurements [Elseifi et al. 2006]. Another 3D finite element model of viscoelastic flexible pavement was validated by Al-Qadi et al. in 2008. Further than

validation, they compared two tire configurations (dual-wheel axle vs. wide-base tire) in three different thickness of HMA layer [Al-Qadi et al. 2008]. Wang and Al-Qadi (2010) studied the responses of a flexible pavement at various tire rolling conditions (free rolling and braking) with a 3D finite element model in Abaqus. They defined the viscoelastic behavior for HMA layer and simulated a loading with a continuous moving load [Wang and Al-Qadi 2010]. In 2012, Khavassefat et al. used a quasi-static procedure to evaluate stresses and strains in viscoelastic model with moving traffic loading. Results of this study showed that the layered elastic analysis used in pavement design is unable to capture several important aspects of pavement responses [Khavassefat et al. 2012].

Because of the improvement in computer technology and software, modeling in general purpose finite element software has been chosen for this study. The pavement structure is modeled in Abaqus/CAE and the responses of this pavement to moving loads are elicited. These responses were compared with responses of the same pavement which is modeled in KENLAYER in purpose of model validation. Since the model is flexible pavement, the two important structural damages are Fatigue Cracking and Rutting. In order to calculate the allowable number of load repetition for each of those distresses, the horizontal tensile strain under the first layer (HMA) and vertical compressive strain on top of the subgrade are needed.

The concentration of this study is based on the responses of flexible pavement. Moreover, a comparison due to moving “Dual-wheel Tandem” and “Tridem” axles loading with different velocities is made. The allowable numbers of load repetition for each of “Fatigue Cracking” and “Rutting” is the parameter which is used for comparison.

Until now, the comparison of different multiple axles have been done using Elastic multilayer analysis without considering the dynamic effects of moving load. In this study the Viscoelastic behavior of HMA were considered. Moreover, all analysis was done by applying moving loads with various speeds. The differences in damages and the advantages of adding an extra axle in tandem configuration instead of adding a tire next to each tires of tandem axles is presented at the end of this paper. In order to be more realistic, the viscoelastic behavior of HMA and moving loads is applied.

2. Methodology

This paper is aimed to using finite element method in 3D model of the pavement structure, analyzing a dynamic loading, which is applied by two different axle configurations. Finally, a comparison between these two types of axles has been made. Two major structural damages are examined for this comparison, fatigue cracking and rutting. The allowable number of load repetition to prevent each of these damages is used as the comparison pa-

rameter. In order to compute distresses, distress models are used, which are introduced in part 2.4. Horizontal tensile strain under HMA layer and vertical compression strain on top of the subgrade are required as the inputs of these models. Each of these inputs is extracted from the analyzed models, the maximum is selected and after an operation which is explained in part 2.4. the results are utilized in the distress models.

Abaqus/CAE is one of the powerful finite element software, which has made modeling a pavement with many realistic assumptions, possible. This software provides a wide variety of material behavior definition that helps the users to model more realistic materials. Some useful assumptions that helped the authors in this study can be named as: a viscoelastic behavior for HMA layer, moving ability for loading parts and modeling infinite parts around the model. Easy modeling and the broad variety of presented responses are the other advantages of using Abaqus/CAE.

2.1 Model Geometry and Material Properties

The model is similar to Wang and Al-Qadi's model [Wang and Al-Qadi 2010] in material properties and layers thickness which has been validated by field measured data. In order to simulate continues pavement situation, a 25 meters longitudinal length and a 10 meters lateral width are modeled. Also, for eliminating the reactions of around supports?

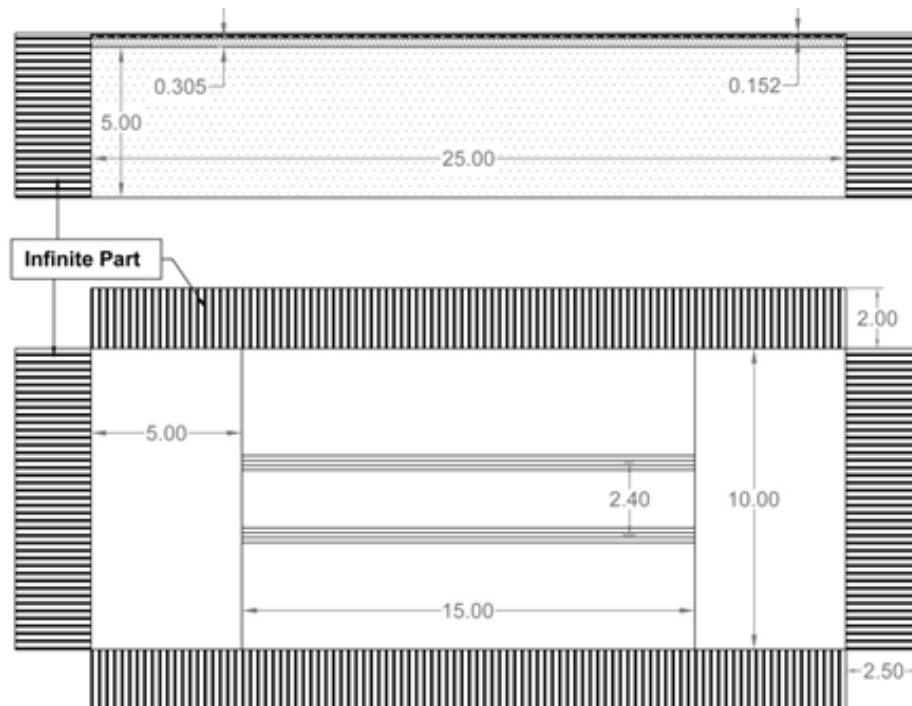


Figure 1. The schematic model geometry

feedback and modeling the far field areas' effect, infinite parts with 2 and 2.5 meter width are added at each end of every layer. The schematic model geometry is shown in Figure 1.

As figure 1 illustrates, the thickness of 152mm, 305mm and 5meter are selected for HMA layer, base and subgrade layer respectively. Two 15 meter thin parallel ribbons, in the middle of the model surface, are considered as the tire path.

For an accurate predict of pavement responses, proper material characterization for each layer is needed. The elastic theory is not able to consider the effect of moving axles while the viscoelastic behavior of asphalt concrete is characterized by the fact that the stress depends on not only the current state of strain but

also the full history of strain development. For defining the viscoelastic phenomena, Prony series are used in material properties. Table 1 illustrates materials properties for each layer.

2.2 Loading and Axles Specifications

As previously mentioned, two types of axle configurations are responsible for applying loads on the pavement structure. The 20 tons load which is diffused on every tire in configuration is carried by the imprint loading areas. These areas' dimensions are calculated through equation (1) and (2):

$$L = \left(\frac{A_c}{0.5227} \right)^{0.5} \quad (1)$$

$$A_c = \pi(0.3L)^2 + (0.4L)(0.6L) = 0.5227L^2 \quad (2)$$

where A_c is the contact area, which can be

Table 1. Elastic and viscoelastic material parameter [Wang and Al-Qadi 2010]

Material	Elastic Parameters		HMA Prony Series at 25°c			
	Resilient Modulus (MPa)	Poisson's Ratio	N	G _i	K _i	τ _i (sec)
HMA Layer	9840	0.35	1	0.6499	0.6499	1E-02
			2	0.2249	0.2249	1E-01
Base Layer	310	0.35	3	0.0852	0.0852	1E+00
			4	0.0246	0.0246	1E+01
			5	0.0171	0.0171	1E+02
Subgrade	262	0.40	6	0.0018	0.0018	1E+03
			7	0.0007	0.0007	1E+04

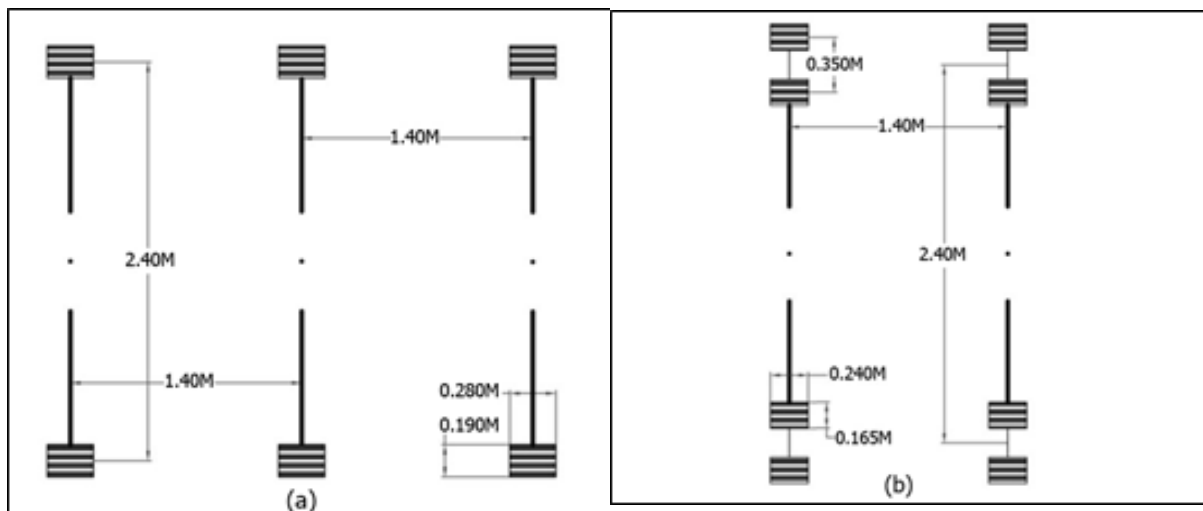


Figure 2. Axle configurations and loading areas dimensions, (a) Tridem Axle, (b) Dual-wheel Tandem Axle

obtained by dividing the load on each tire by the tire pressure. A rectangular loading area is assumed with length $0.8712L$ and width $0.6L$ which has the same area of $0.5227L^2$ [Huang 2004]. On the other side, the tire pressure is opted 90psi (621KPa) and applied uniformly on the imprint areas.

Axle configurations are modeled in standard dimensions, 1.4 meter spacing between every axles and 2.4 meter length of each axle which is illustrated in Figure 2. The spacing between

dual-wheels is considered 350mm.

According to research studies done, changes in inflation pressure by changing the speed parameter are approximately 5% and are negligible [Chatti et al. 1996]. Thus, considering the constant pressure for tires at each speed causes equal contact area.

2.3 Finite Element Specifications

Because of the model's large dimensions and the 3D modeling the required elements are nu-

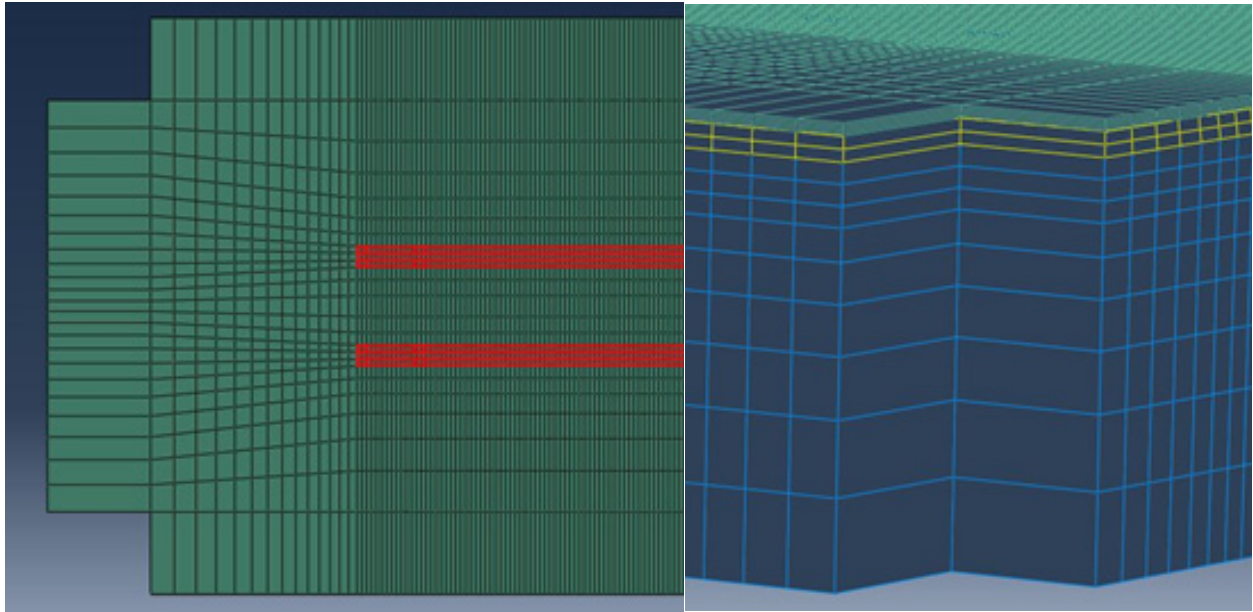


Figure 3. Increasing in elements size by getting far from loading area, (a) in horizontal surface, (b) in depth of pavement

merous and a management of them is necessary in order to control the run time. For this management, two parallel ribbons are defined as the wheels paths and meshed by smaller elements. Moreover, the elements sizes are increased by getting far from the loading part. The elements horizontal dimensions around these wheel paths are 18mm laterally and 12mm in moving direction. The vertical elements dimensions for every layer from top to down for HMA, base and subgrade layer are 30.4mm, 152mm and 152-1200mm respectively. The change in elements dimensions is illustrated in Figure 3.

Two types of elements are used in this model: eight-node linear brick elements with reduced integration (C3D8R) in every normal part, and infinite elements (CIN3D8) at the end of every layer. Infinite parts are used to reduce the

number of far field elements without significant loss in responses' accuracy and in order to create "silent" boundaries for the dynamic analysis [Abaqus Users' Manual 2010].

2.4 Distress Models

In order to represent the damage parameter, distress models are used for calculating the allowable number of load repetition to prevent fatigue cracking and rutting. The Asphalt Institute (AI) introduced these two models which are presented in Equations (3) and (4) [Huang 2004]:

$$N_f = 0.0796 \times (\epsilon_t)^{-3.291} \times (E)^{(-0.854)} \quad (3)$$

$$N_d = 1.365 \times 10^{-9} \times (\epsilon^c)^{-4.477} \quad (4)$$

where N_f is the allowable load repetition to prevent fatigue cracking and N_d is the allowable load repetition to prevent permanent deformation (rutting); E is the elastic modulus of

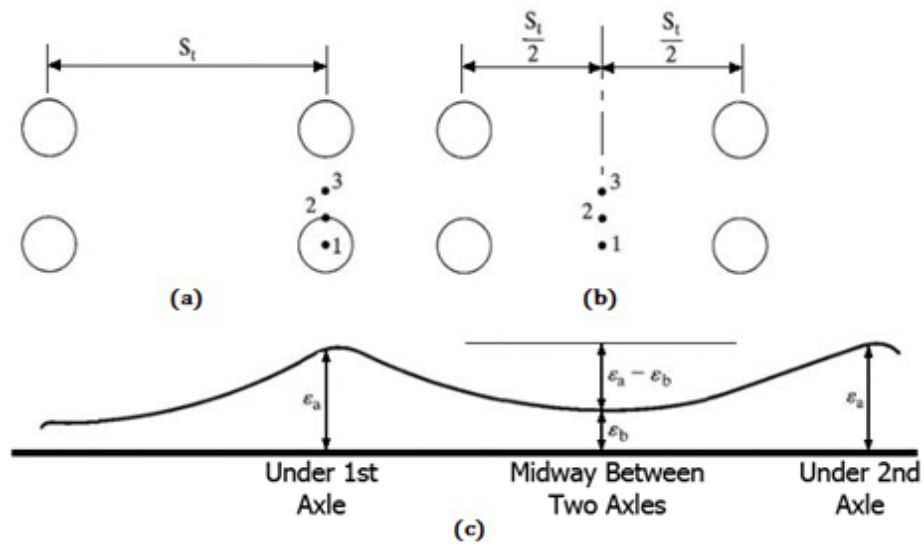


Figure 4. Strain data for distress models [Huang 2004]

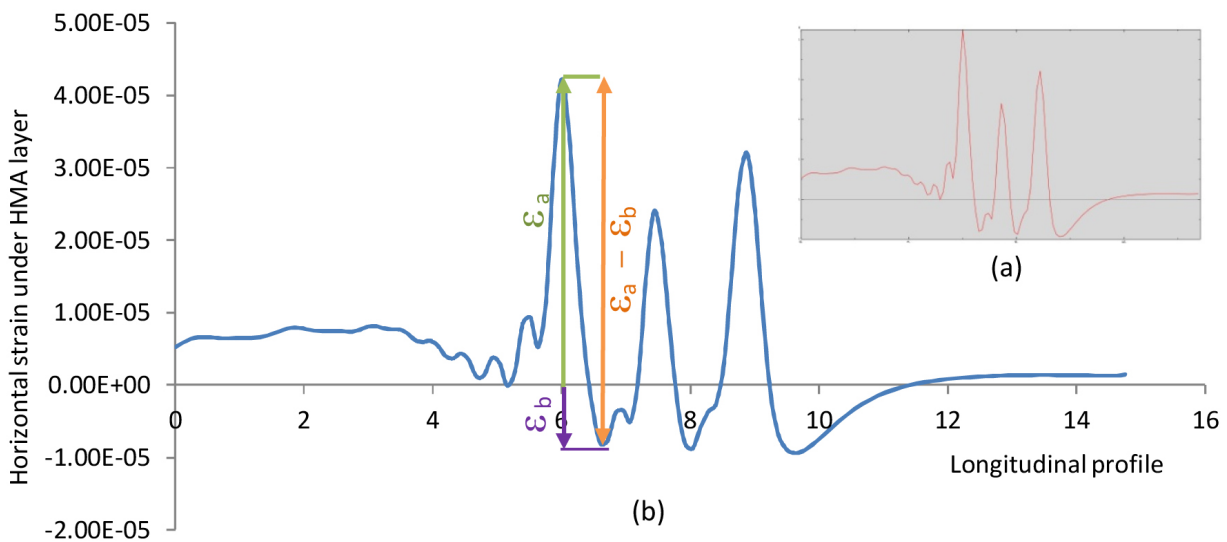


Figure 5. Finding the maximum strain for inputs of distress model; The Abaqus exported diagram (a) does not have a high quality, so the numerical diagram has been provided by Microsoft Office Excel (b).

AC layer which can be eliminated because of its small power compared with strain's power; ϵ_t is tensile horizontal strain under HMA layer and ϵ_c is vertical compressive strain on top of the subgrade. For multiple axles, computing these strains are slightly different, the maximum strain should be selected from the strains

under each axle (as shown in Figure 4a.) and strains at the corresponding points that lies midway between two axles (as shown in Figure 4b.). [Huang 2004]

Selecting the maximum of ϵ_a , ϵ_b and $\epsilon_a - \epsilon_b$ is necessary for finding the true input for each model. Figure 5 shows the tensile horizontal

strain under the first layer in axles moving direction, the Abaqus exported diagram (Figure 5a) illustrates on top of the numerical diagram (Figure 5b). Apparently if ϵ_a and ϵ_b have the same sign (either positive or negative), $\epsilon_a - \epsilon_b$ could not be higher than each of them. Two lateral and longitudinal horizontal strains should be investigated to select the maximum input for fatigue damage model.

3. Results and Discussion

3.1 Pavement Responses and Damage Analysis

Calculating the allowable number of load repetition to prevent fatigue cracking requires extracting horizontal strains under HMA layer in two perpendicular directions. The extracted

strains (after the operation defined in part 2.4) and the model's responses for each direction's strains are presented in Table 2. The last row of Table 2 is the minimum of both directions' function's response. In order to make comparison easier, Figure 6 illustrates Table 2's contents.

A comparison between horizontal strains under HMA layer shows that with the Dual-wheel Tandem axle passage, higher strains in moving direction are generated. While the generated strains in lateral direction is higher by passage of Tridem axle configuration. The lower strains in lateral direction due to passed Dual-wheel Tandem axle are because of the interaction between each tire response on the

Table 2. The allowable number of load repetition to prevent fatigue cracking

Strain Direction	Axle type	Tridem Axle				Dual-wheel Tandem Axle			
	Axle Speed (km/h)	20	60	80	100	20	60	80	100
In axle's moving direction	Max strain for Fatigue Distress Model (*E-4)	1.036	0.941	0.972	0.956	1.201	1.118	1.137	1.131
	N_{f1} (*E+12)	1.035	1.417	1.276	1.342	0.635	0.802	0.761	0.772
In lateral direction	Max strain for Fatigue Distress Model (*E-4)	0.939	0.770	0.751	0.720	0.703	0.642	0.635	0.628
	N_{f2} (*E+12)	1.428	2.744	2.981	3.416	3.702	4.992	5.177	5.374
Min $N_{f1,2}$ (*E+12)		1.035	1.417	1.276	1.342	0.635	0.802	0.761	0.772

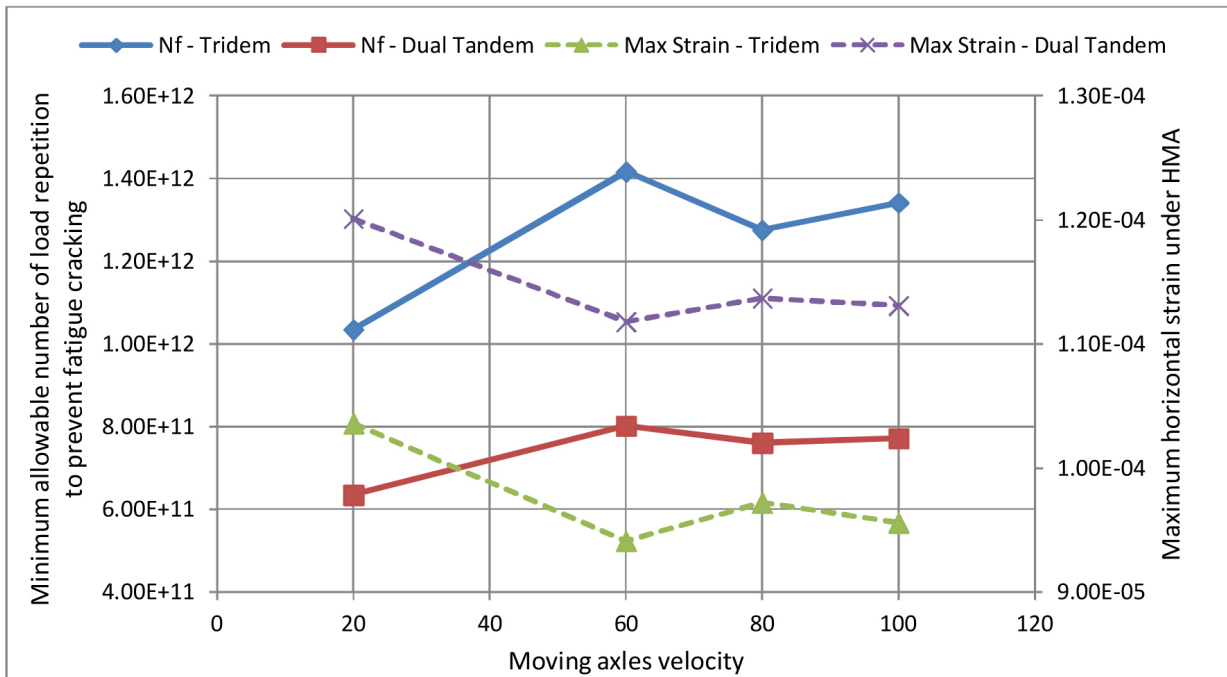


Figure 6. Minimum allowable number of load repetition to prevent Fatigue Cracking

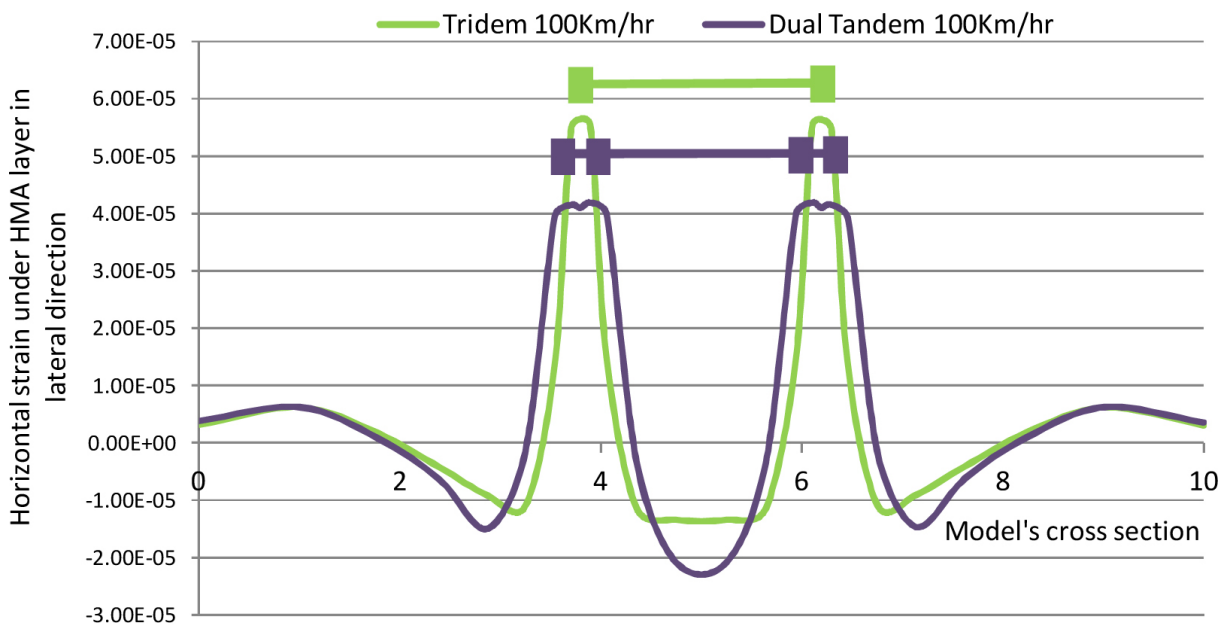


Figure 7. Sample of horizontal strains in lateral direction due to passage of two axle configurations

other one. The small spacing between a pair of tires causes the neutralization of pavement responses to each tire and also causes the reduction in maximum strains under dual wheels.

A lateral profile of strains under HMA layer generated by the passage of these two axle configuration has been presented in Figure 7. As Figure 7 shows, not only the tensile strains

(positive part of strain diagram) caused by Dual-wheel Tandem axle passage are lower than the one created by Tridem axles passage, but also the compressive strain (negative part of strain diagram) in axles' midway point caused by Dual Tandem axles is greater than the one Tridem axles have made. The reason of this event is higher loading in each axle of the Dual-wheel Tandem in comparison to Tridem axles which creates higher strains in this point. Generally, the higher loading on each axle has greater responses in the midway of large distances. This is the cause of higher strains in moving direction by Dual-wheel Tandem axles in comparison to Tridem axles. Hence the larger length of each axle versus the spacing between axles (2.4m vs. 1.4m) caused the higher strain in moving direction. There-

fore, the determinant strain for computing the distress model of fatigue cracking is “in moving direction strain” and because of this fact, the Dual-wheel Tandem configuration is making more fatigue cracking distresses. In other words, as Figure 6 illustrates, allowable number of Tridem axle configuration passage to prevent fatigue cracking is higher than Dual-wheel Tandem axles.

The effect of axles' velocity and the dynamic loading is another output of this diagram. The speed of 20km/h has made higher strains in the diagram's range of speed and it is because of the dominant static effect of loading at low speeds. Generally, the summation of load's static effects and load's dynamic effects is influencing in the responses. By increasing the velocity, dynamic effect and static load's ef-

Table 3. Allowable number of load repetition to prevent Fatigue cracking

Strain Direction	Axle type	Tridem Axle				Dual-wheel Tandem Axle			
	Axle Speed (km/h)	20	60	80	100	20	60	80	100
In axle's moving direction	Max strain for Fatigue Distress Model (*E-4)	1.036	0.941	0.972	0.956	1.201	1.118	1.137	1.131
	N_{f1} (*E+12)	1.035	1.417	1.276	1.342	0.635	0.802	0.761	0.772
In lateral direction	Max strain for Fatigue Distress Model (*E-4)	0.939	0.770	0.751	0.720	0.703	0.642	0.635	0.628
	N_{f2} (*E+12)	1.428	2.744	2.981	3.416	3.702	4.992	5.177	5.374
Min $N_{f1,2}$ (*E+12)		1.035	1.417	1.276	1.342	0.635	0.802	0.761	0.772

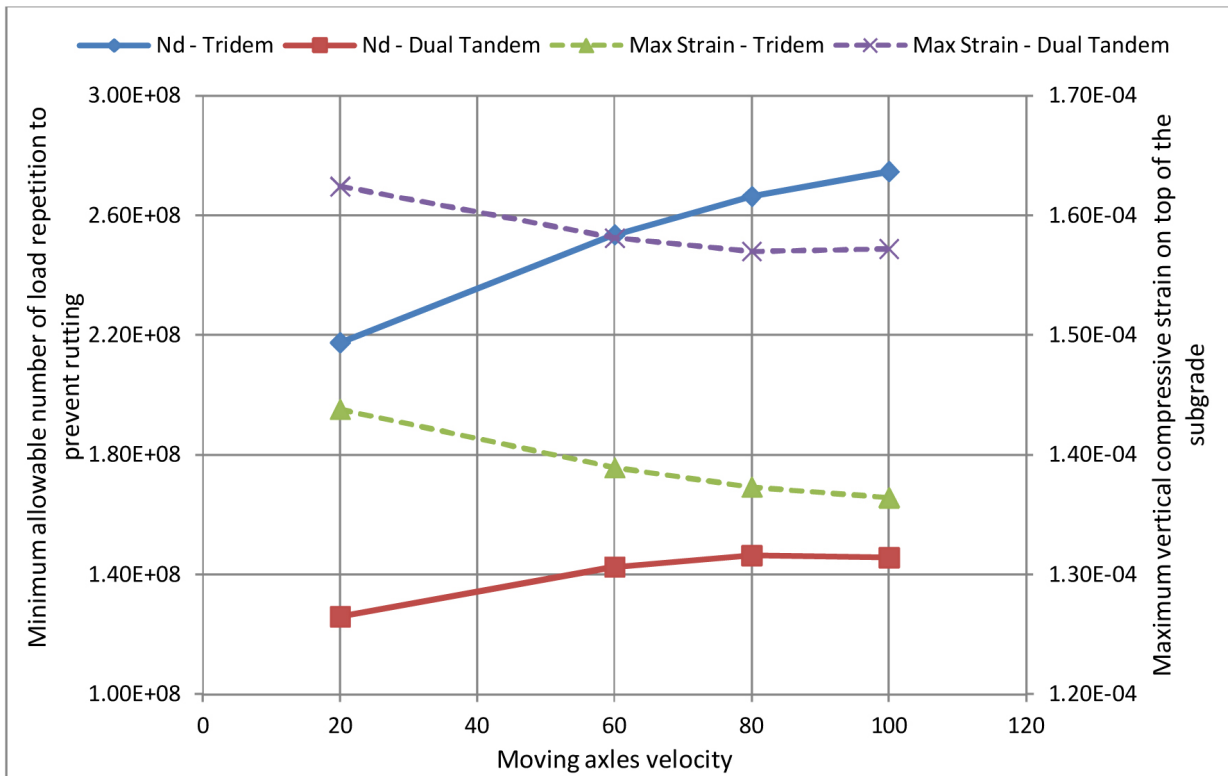


Figure 8. Allowable number of load repetition to prevent Rutting damage

fect reverse their influence; the static effect is decreasing but its role is considerable up to a velocity around 80km/h. This speed is the local extremum point of the diagram which the summation of both dynamic and static load's effect is higher than other points, although it is not higher than load's static effect in low speeds.

In order to calculate allowable number of load repetition to prevent Rutting, extracting the vertical compressive strains on top of the subgrade is required. The vertical strains on top of the subgrade are totally compressive and they have same signs, so, the operation is not required (as it was explained in 2.4). Table 3 is presenting the net strains and the distress

model's response to these strains. Further, figure 8 illustrates an easier comparison diagram for contents of Table 3.

As Figure 8 illustrates, because of the deeper position of the extracted data and the effects of layer's weight, the load's dynamic effect is less considerable than its effect under HMA layer. Hence, when the velocity increases higher than 60km/h, low decrease in strain responses is observed.

In order to determine the loading area as the imprint of tires, the appointed load (20 ton) is divided to number of each configuration's tires. Therefore, the total load which is carried by each axle of the Tridem configuration is less than this load on each axle of Dual-wheel

Tandem configuration (6 tires vs. 4 pairs of tires). According to this fact, the vertical compressive strains (which is directly related to stresses) under Dual-wheel Tandem axles are much greater than this response under Tridem axles. By this explanation, the major number of allowable load repetition to prevent rutting damage due to Tridem axles passage is expectable.

3.2 Validation

Wang and Al-Qadi have presented a valid model. Their model was simulated in Abaqus, and validated by field measured data [Wang and Al-Qadi 2010]. As previously mentioned, the basic specifications of this study's model are similar to Wang and Al-Qadi's model. The field measured validation results of Wang and Al-Qadi's model verifies the model utilized in this study.

Moreover, quantitative evaluation has been

made using KENLAYER software. KENLAYER is a commonly used software in pavement analysis which utilizes elastic layer theory and is endorsed for pavement structure design. A Tridem axle model with static loading is analyzed by Abaqus and has been utilized for comparing with the same model in KENLAYER program. Extracted data from each software is presented in Table 4 in order to compare and compute the percentage difference.

4. Discussion and Conclusion

Modeling a 3D pavement in general purpose finite element software (Abaqus/CAE) and analyzing its outputs was the approach of this paper. The pavement responses caused by the passage of two different axle configurations with four different velocities were used in order to calculate damage transfer functions under these conditions. In simulating stud-

Table 4. Comparison between ABAQUS and KENLAYER responses

Extracted Response	Position	ABAQUS	KENLAYER	Percentage difference
Vertical Displacement (mm)	On top of HMA	0.179	0.177	0.96%
Vertical Displacement (mm)	On top of Subgrade	0.128	0.124	3.05%
Vertical Stress (KPa)	On top of HMA	583.13	622.70	6.35%
Vertical Stress (KPa)	On top of Subgrade	32.83	30.04	9.30%
Tensile Horizontal Strain	Under HMA Layer	7.16E-5	7.93E-5	9.71%
Vertical Strain	On top of HMA	1.87E-5	1.75E-5	11.97%
Vertical Strain	On top of Subgrade	1.18E-4	1.06E-4	11.32%

ies, simplifications are inevitable. Software constrains and unnecessary calculations are the main reasons of these assumptions. In this study, simplification in modeling the loading area in rectangular shape was made which is recommended by Huang [Huang2004]. Neglecting the roughness of surface caused higher amount of load repetition. The smooth surface applied because of limited ability of computers to analysis the complex model and unnecessary calculation. Hence, only the comparison between results is used for conclusion.

The following conclusions were drawn from this study:

- The Dual-wheel Tandem configuration of tires creates higher critical stains in pavement in comparison with Tridem axle configuration. Hence fewer numbers of load repetitions by Dual-wheel Tandem causes structural damages (Fatigue Cracking and Rutting). Finally, the superiority of adding an extra axle in Tandem configuration instead of adding a tire next to each tire of Tandem axles has been concluded.
- The effect of dynamic loading and axles' velocity was illustrated in this study. Increasing velocities up to 100km/h caused the reduction in responses. Because of greater static's effect of loading, this reduction in lower speeds is more than higher speeds. Increasing velocities make the dynamic's effects of loading more than static's effect of that, although it cannot

be higher than load's static's effect in low speeds.

- The behavior of horizontal strains due to the passage of Dual-wheel Tandem axles and Tridem axles in the depth of 152mm of the pavement (under HMA layer's thickness) becomes inverse with direction alteration. Tridem axles create higher lateral horizontal strains under HMA layer, while this configuration makes lower horizontal strain in axles' moving direction. The difference of loading spacing in each direction and loads magnitude on each axle is the causes of this disaccord.

5. References

- Abaqus Vesion 6.10, User's Manual, 2010.
- Akram, T., Scullion, T., Smith, R. E. and Fernando, E. G. (1992) "Estimating damage effects of dual versus wide base tires with multi depth deflectometers", Transportation Research Record, No. 1355, TRB, National Research Council, Washington, DC, pp. 59-66.
- Al-Qadi, I. L., Wang, H., Yoo, P. J. and Des-souky, S. H. (2008) "Dynamic analysis and in situ validation of perpetual pavement response to vehicular loading", Journal of the Transportation Research Board, Transportation Research Board of the National Academies, Washington, D.C., pp. 29-39.

- Chatti, K., Kim, H. B., Yun, K. K. and Monismith, C. L. (1996) "Field investigation into the effects of vehicle speed and tire pressure on asphalt concrete pavement strains", Transportation Research Record, No.1539, TRB, Washington, D.C., pp. 66-71.
- Chen, C. H., Marshek, K. M. and Saraf, C. L. (1990) "Effect of truck tire contact pressure distribution on the design of flexible pavement: A three-dimensional finite element approach", Transportation Research Record, No. 1095, pp. 72-78.
- Dondi, G. (1994) "Three-dimensional finite element analysis of a reinforced paved road", Fifth International Conference on Geotextiles, Geomembrane and Related Products, Vol. 11, Singapore 1994, pp. 95-100.
- Elseifi, M. A., Al-Qadi, I. L. and Yoo, P. J. (2006) "Viscoelastic modeling and field validation of flexible pavements", Journal of Engineering Mechanics, ASCE, Vol. 132, No. 2, pp. 172-178.
- Hjelmstad, K. D., Kim, J. and Zuo, Q. H. (1997) "Finite element procedures for three-dimensional pavement analysis", Proceedings of the 1997 Airfield Pavement Conference, ASCE, Seattle, Washington, USA, pp. 125-137.
- Huang, Y. H. (2004) "Pavement analysis and design", Pearson Prentice Hall, Upper Saddle River N.J.
- Khavassefat, P., Jelagin, D. and Birgisson, B. (2012) "A computational framework for viscoelastic analysis of flexible pavement under moving loads", Journal of Materials and Structures, Rilem, Vol. 45, pp. 1655-1671.
- Saad, B., Mitri, H. and Poorooshab, H. B. (2005) "Three-dimensional dynamic analysis of flexible conventional pavement foundation", Journal of Transportation Engineering, ASCE, Vol. 131, pp. 460-469.
- Sebbaly, P. E. and Tabatabaee, N. (1993) "Influence of vehicle speed on dynamic loads and pavement response" Transportation Research Record, No. 1410, TRB. Washington D.C., pp. 107-114.
- Uddin, W., Zhang, D. and Fernandez, F. (1994). "Finite element simulation of pavement discontinuities and dynamic load response." Transportation Research Record 1448, TRB, National Research Council, Washington, D.C., pp. 100-106.
- Wang, H. and Al-Qadi, I. L. (2010) "Evaluation of surface-related pavement damage due to tire braking", Asphalt Pavement and Environment, Taylor and Francies, Vol. 11, No. 1, pp. 101-121.

- Zaghoul, S. M. and White, T. D. (1993)
“Use of a three-dimensional, dynamic finite element program for analysis of flexible pavement”, Transportation Research Record, No. 1388, National Research Council, Washington D.C. pp. 60-69.